Beam Dynamics Challenges for the ILC

Stanford Linear Accelerator Center, Stanford University, Stanford, CA 94309

Beam Dynamics Challenges for the ILC

Kiyoshi Kubo, KEK, 1-1 Oho, Tsukuba, Ibaraki 305-0801 Japan
Mail to: kiyoshi.kubo@kek.jp

Andrei Seryi, SLAC, 2575 Sand Hill Road, Menlo Park, CA 94025 USA
Mail to: seryi@slac.stanford.edu

Nicholas Walker, DESY, Notkestrasse 85, 22607 Hamburg, Germany
Mail to: nicholas.walker@desy.de

Andy Wolski, The Cockcroft Institute, Daresbury, Warrington WA4 4AD, UK
Mail to: a.wolski@dl.ac.uk

2.1.1   Introduction

The International Linear Collider (ILC) is a proposal for 500 GeV centre-of-mass electron-positron collider, with a possible upgrade to ~1 TeV centre-of-mass. At the heart of the ILC are the two ~12 km 1.3 GHz superconducting RF (SCRF) linacs which will accelerate the electron and positron beams to an initial maximum energy of 250 GeV each. The Global Design Effort (GDE) – responsible for the world-wide coordination of this uniquely international project – published the ILC Reference Design Report in August of 2007 [1].

The ILC outlined in the RDR design stands on a legacy of over fifteen-years of R&D. The GDE is currently beginning the next step in this ambitious project, namely an Engineering Design phase, which will culminate with the publication of an Engineering Design Report (EDR) in mid-2010.

Throughout the history of linear collider development, beam dynamics has played an essential role. In particular, the need for complex computer simulations to predict the performance of the machine has always been crucial, not least because the parameters of the ILC represent in general a large extrapolation from where current machines operate today; many of the critical beam-dynamics features planned for the ILC can ultimately only be truly tested once the ILC has been constructed. It is for this reason that beam dynamics activities will continue to be crucial during the Engineering Design phase, as the available computer power and software techniques allow ever-more complex and realistic models of the machine to be developed. Complementary to the computer simulation efforts are the need for well-designed experiments at beam-test facilities, which – while not necessarily producing a direct demonstration of the ILC-like parameters for the reasons mentioned above – can provide important input and benchmarking for the computer models.

The fundamental challenge for the ILC beam dynamicists is the production and preservation of the ultra-small emittance beams required for the ambitious luminosity goal of $\sim 2 \times 10^{34}$ cm^{-2}s^{-1}. A general scaling law for the luminosity for a fixed centre-of-mass energy can be written as

$$L \propto P_{beam} \sqrt{\frac{\delta_{RMS}}{\varepsilon_y}} \,, \tag{1}$$

where P_{beam} is the average beam power, δ_{RMS} is the RMS energy loss of the beams during the collision (beamstrahlung), and ε_y is the normalized vertical emittance. Implicit in the scaling law are the assumptions of a flat beam ($\varepsilon_x >> \varepsilon_y$) and that the vertical beta-function at the interaction point (β_y^*) is constrained by the bunch length (σ_z) such that $\beta_y^* \geq \sigma_z$ to avoid the so-called "hour-glass" effect leading to a loss of luminosity. Assuming that we constrain the beamstrahlung to a fixed few percent[1], achieving a high luminosity requires high beam powers (current), ultra-small vertical emittance beams, short bunch lengths and very strong focusing at the interaction point. Some examples of the nominal ILC parameters are given in Table 1.

Table 1: Typical key parameter ranges for the 500 GeV centre-of-mass ILC

	min.	*nominal*	*max.*	
Bunch population	1	2	2	$\times 10^{10}$
Number of bunches	1260	2670	5340	
Linac bunch interval	180	369	500	Ns
RMS bunch length at IP	200	300	500	μm
Normalized horizontal emittance at IP	10	10	12	mm·mrad
Normalized vertical emittance at IP	0.02	0.04	0.08	mm·mrad
Horizontal beta function at IP	10	20	20	Mm
Vertical beta function at IP	0.2	0.4	0.6	Mm
RMS horizontal beam size at IP	474	640	640	Nm
RMS vertical beam size at IP	3.5	5.7	9.9	Nm
Vertical disruption parameter	14	19.4	26.1	
Fractional RMS energy loss to beamstrahlung	1.7	2.4	5.5	%

Achieving these ambitious parameters requires pushing the envelope in every sub-system of the ILC. Figure 1 shows the layout (footprint) of the machine, indicating the main sub-systems:

- The electron and positron sources must produce the necessary bunch charge and train structure (2670 bunches in a ~950 μs pulse). The electron source must produce a high (~90%) level of polarisation, using a laser-driven photo-injector and a GaAs cathode. Positrons are produced by using an undulator magnet in the main electron linac to produce high energy photons (gammas), which then impact a thin Ti-alloy target to produce electron positron pairs. This positron source can also be used to generate polarized beams. In both cases, the beams must be efficiently captured and accelerated to 5 GeV before being injected into the damping rings.
- The electron and positron damping rings are centrally located. The two 6.7 km circumference storage rings are responsible for producing the high-

---

[1] For both physics reasons and suppression of beam-beam backgrounds

quality ultra-small emittance beams required by the luminosity: achieving the required 2 pm vertical emittance is the primary challenge. To do so they must damp the vertical emittances by (in the case of the positrons) approximately eight orders-of-magnitude in the 200 ms storage time. Many of the fundamental beam dynamics challenges for the ILC are associated with the damping rings, particularly collective effects, both classical and in particular electron-cloud and fast-ion instability effects.

- The Ring to Main Linac section (RTML) must transport the ejected beams from the damping rings, along the entire length of the main linacs, where they are turned around and injected into the bunch compressors, and simultaneously accelerated from 5 GeV to ~15 GeV before being injected into the main linacs. Bunch compression by a factor of ~30 is achieved in two stages by rotating the longitudinal phase space. SCRF linacs are used to introduce a strong energy correlation along the bunches, which enable non-isochronous magnetic chicanes to compress the bunch longitudinally. The primary beam dynamics concern here is the preservation of the tiny vertical emittance during transport and bunch compression. Many of the fundamental problems of wakefields and chromatic effects are essentially the same as in the main linacs (see below), but are exacerbated by the very long bunch before and the large energy spread after compression.

- The Main Linac is essentially a repetitive system of SCRF accelerating structures with focusing provided by a simply FODO lattice structure. As with the RTML, the primary beam dynamics issues related to emittance preservation. Suppression of higher-order modes (HOMs, or long-range wakefields) is achieved by random cavity detuning of the HOMs and by HOM-couplers and absorbers mounted in the accelerating units (cryomodules). Short range (single-bunch) wakefields of the large-iris superconducting cavities are relatively weak, and so the primary emittance growth arises from chromatic effects and cross-plane coupling arising from the alignment errors of the quadrupole lattice.

- The Beam Delivery System (BDS) is responsible for transporting the high-energy beams from the linacs to the interaction region, where they are strongly focused to the required nanometer-size beams at the collision point. This challenges the optics of the Final Focus system, which requires careful cancellation of second- and higher-order chromatic and geometric aberrations. In addition, the strong focusing (small β_y^*) places extremely tight component alignment and field-quality tolerances on the magnets. Magnet vibration and slow ground motion issues must be considered, and keeping the tiny beams in collision at the IP will require fast beam-based feedback systems.

Each sub-system has its unique set of beam dynamics issues. For the remainder of this report, we will focus specifically on a summary of the issues in the Damping Ring, the RTML and Main Linac and in the final section the BDS. For more detailed and comprehensive list of beam dynamics challenges for the ILC (including the sources), the reader is referred to the RDR and the references therein [1].
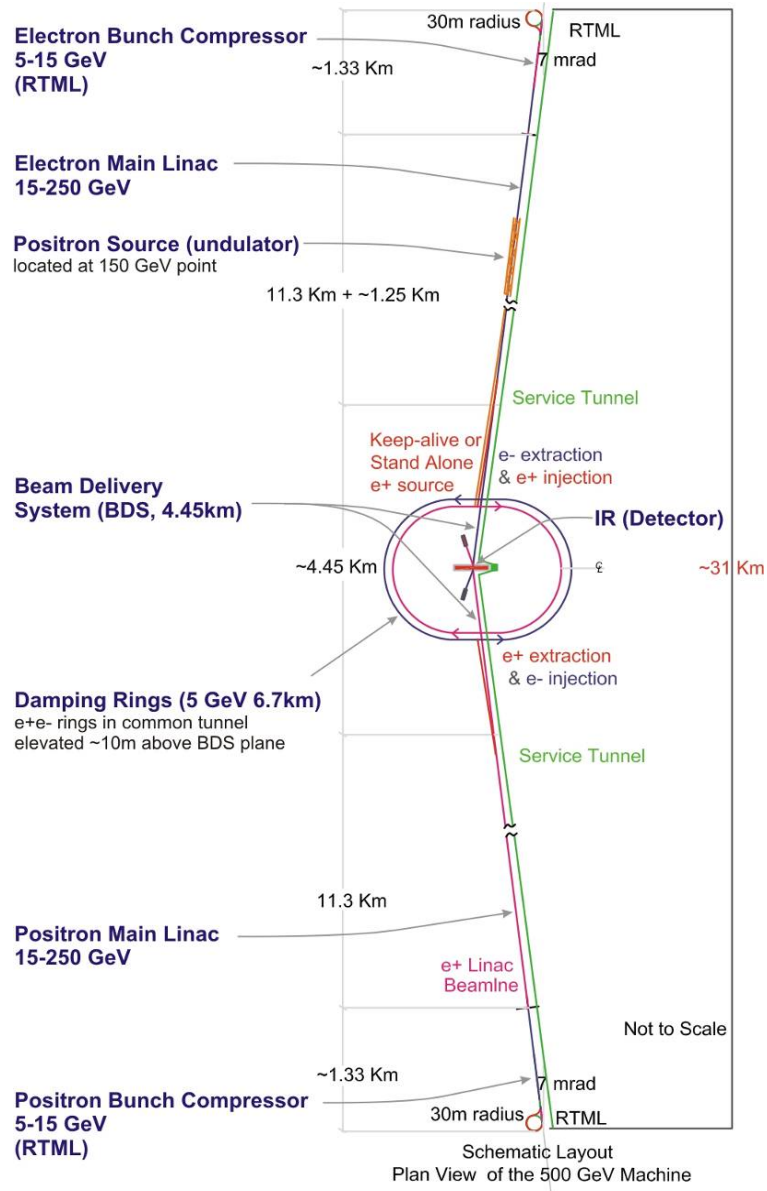
Figure 1: Schematic layout of the 500 GeV centre-of-mass ILC.

2.1.2 Damping Rings

   Generation of luminosity in the ILC will depend on colliding beams with emittances much smaller than can be produced directly from particle sources. In the case of the positron beam, the vertical emittance must be reduced by five orders of magnitude between the source and the interaction point. Emittance reduction is achieved by radiation damping, with each beam remaining in a synchrotron storage ring (damping ring) for 200 ms between machine pulses. The principal parameters of the damping rings must be chosen to provide a balance between competing requirements. For example, the circumference must be large enough to accommodate a full train of up to

around 6000 bunches, with sufficient spacing between bunches to fire the injection and extraction kickers; however, increasing the circumference leads to longer damping times, increases the impact of some beam dynamics effects such as space charge, and increases the costs of the rings. The higher the energy of the stored beam, the shorter the damping times and the more robust the beam will be against various collective effects; however, raising the beam energy also increases the equilibrium emittances, and increases the cost of the damping rings. An analysis [2] taking into account a range of considerations has led to the present damping ring design having circumference of about 6.5 km, and beam energy of 5 GeV.

The principal beam dynamics issues in the damping rings are: achieving high injection efficiency of the large-emittance positron beam (with average injection power 225 kW); tuning for ultra-low vertical emittance; and maintaining beam quality and at high bunch charges and average currents. Regarding injection efficiency, the dynamical effects of intrinsic nonlinearities in the field of the damping wigglers are a concern, and have been the subject of detailed study. The present belief is that sufficiently good field quality can be achieved in the wigglers such that limitations on dynamic aperture will come from other sources. Some of the techniques applied in the studies leading to this conclusion have been described previously [3], and we do not elaborate further here. In this article, we discuss briefly the issues associated with achieving vertical emittance of less than 2 pm, and some of the many effects that threaten to impact beam stability.

While the horizontal emittance in a storage ring is generally determined by the lattice design, the vertical emittance is usually limited by magnet alignment and tuning errors that generate vertical dispersion and betatron coupling. The non-zero opening angle of the synchrotron radiation in a storage ring imposes a fundamental lower limit on the vertical emittance, since there is some vertical momentum recoil when particles in the beam emit photons. Neglecting other effects (dispersion and betatron coupling) that generate vertical emittance, the equilibrium emittance determined from the opening angle of the synchrotron radiation can be calculated for a given lattice using the formula:

$$\varepsilon_y = \frac{13}{55} \frac{C_q}{j_y} \frac{\oint \beta_y / |\rho|^3 \, ds}{\oint 1/\rho^2 \, ds} \tag{2}$$

where C_q is the quantum constant ($\approx 3.832 \times 10^{-13}$ m), j_y is the vertical damping partition number, β_y is the vertical beta function, and $1/\rho$ is the curvature of the reference trajectory. Note that this expression is independent of beam energy: although higher-energy particles emit photons with higher momenta for a given bending radius, the opening angle of the radiation is reduced at higher beam energy. Generally, one finds for damping ring designs that the vertical emittance given by Eq. (2) is of order 0.1 pm, while the specified equilibrium vertical emittance is 2 pm: we expect that in practice, the vertical emittance will be dominated by magnet alignment errors.

In the ILC damping rings, the target vertical emittance of 2 pm is about 0.25% of the specified horizontal emittance; correction of betatron coupling at this level has been demonstrated at existing storage rings. However, the contribution of vertical dispersion to the vertical emittance is likely to be as important as that from betatron coupling. If the vertical dispersion is generated by random, uncorrelated errors around a storage ring, then the contribution of the vertical dispersion to the vertical emittance can be estimated from:

$$\varepsilon_y \approx 2 j_z \left\langle \frac{\eta_y^2}{\beta_y} \right\rangle \sigma_\delta^2 \qquad (3)$$

where j_z is the longitudinal damping partition number, η_y is the vertical dispersion, σ_δ is the rms energy spread, and the brackets $\langle\rangle$ indicate an average around the ring. Applied to the ILC damping rings, we find that the rms vertical dispersion in the damping rings needs to be less than 3 mm, without any allowance for betatron coupling. Assuming that at the specified vertical emittance betatron coupling and vertical dispersion make roughly equal contributions to the vertical emittance (as suggested by simulations), the betatron coupling must be less than about 0.1%, and the rms vertical dispersion must be less than about 1.5 mm. Based on experience at operating storage rings, these figures indicate that the goal of 2 pm vertical emittance in the ILC damping rings is realistic; however, the lowest vertical emittance demonstrated to date is about a factor of two larger than this [4]. Further studies are needed to demonstrate tuning techniques that are sufficiently effective and can be applied quickly in a machine of the size and complexity of the damping rings. Initial alignment of magnets, functionality and performance of diagnostics (particularly beam position and beam size monitors), and application of beam-based alignment techniques will all be critical. Once achieved, the vertical emittance will be sensitive to motion of the sextupoles at the level of tens of microns; so mechanical and thermal stability of the damping ring components and their environment will also be critical issues.

One feature that will distinguish the ILC damping rings from most storage rings built to date is that around 80% of the synchrotron radiation will come from the damping wiggler: in third generation synchrotron light sources, insertion devices typically account for around 20% of the radiation. The present design of the ILC damping rings includes about 140 m of wiggler with peak field 1.6 T, so as to achieve damping times of less than 25 ms. One consequence of the fact that the wigglers dominate the radiation loss is that for tuning the vertical emittance, particular attention must be paid to correction of dispersion and local betatron coupling in the wiggler sections. This may allow some improvements in speed and efficiency of low-emittance tuning if global correction strategies (for example, orbit response matrix analysis) are modified to act locally.

Correction of errors at the level necessary to achieve 2 pm vertical emittance is essentially an issue of single-particle dynamics. However, the damping rings will need to operate with average currents of 400 mA, and bunch charges of up to 3 nC; with these parameters, a range of collective effects threaten to limit beam quality and stability. Effects that are of concern include: space-charge tune shifts; intrabeam scattering; impedance; ion instabilities (in the electron damping ring); and electron cloud effects (in the positron damping ring). Coherent synchrotron radiation has also been considered, but is not thought likely to have a significant impact with the present configuration. The effect causing most concern, based on present understanding and experience from other facilities, is electron cloud [5].

Instabilities associated with electron cloud have been observed in a number of proton and positron storage rings. A key mechanism associated with the build-up of electrons in the vacuum chamber of a proton or positron ring is the release of secondary electrons from the impact of primary electrons on the chamber wall. Although the secondary electrons are at low energy, a positively charged beam can accelerate them to energies where they can themselves release multiple secondary electrons on striking the

wall. Depending on the beam parameters, properties of the vacuum chamber surface, and presence of external electromagnetic fields, multipacting can lead to a rapid increase in the density of electrons in the chamber, with saturation occurring when the charge on the beam is effectively neutralized by the charge on the electrons in the cloud. Figure 2 shows the results of a simulation of the variation in density of the electron cloud in the wiggler of the positron damping ring, during the passage of three bunches of positrons. As a bunch passes, electrons in the cloud are accelerated and hit the wall with high energy, releasing showers of secondary electrons, and resulting in an increase in the cloud density; between bunches, the cloud dissipates. At sufficiently high electron densities, interactions between the cloud and the beam can lead to a variety of undesirable effects, including incoherent tune shifts, emittance growth, and instabilities. Figure 2 shows the results of a simulation of the vertical beam size in the positron damping ring, over 1000 turns, starting from the nominal beam parameters, and with various densities of electron cloud (averaged around the ring). Up to densities of around 1.2×10^{11} m^{-3}, there is no significant increase in the beam size; above densities of 1.4×10^{11} m^{-3}, the interaction between the cloud and the beam drives a weak instability that increases the beam emittance.
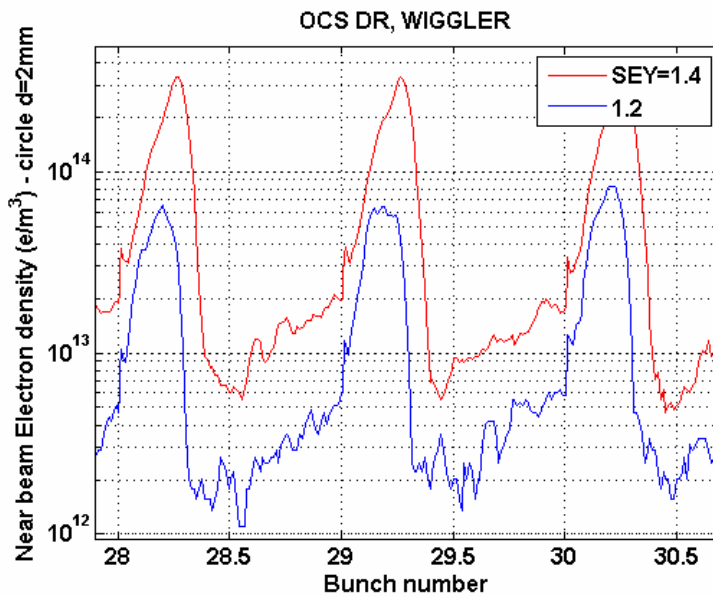

Figure 2: (M. Pivi, SLAC) Variation of near-beam electron cloud density in the wiggler section of the ILC positron damping ring. Cases with peak secondary electron yield 1.2 (blue line) and 1.4 (red line) are shown.

The electron cloud research program for the ILC damping rings has two goals: first, to determine the maximum density of electrons in the chamber before there is an adverse impact on the beam quality and stability; and second, to demonstrate effective and practical techniques for suppressing the development of electron cloud, so that the electron density stays at safe levels. Figure 3 compares the predicted instability threshold, with the expected cloud density under various conditions. While it seems likely that conditions can be found to avoid any effects from electron cloud, the significant uncertainty in the simulation results makes it desirable to aim for a significant margin of safety.
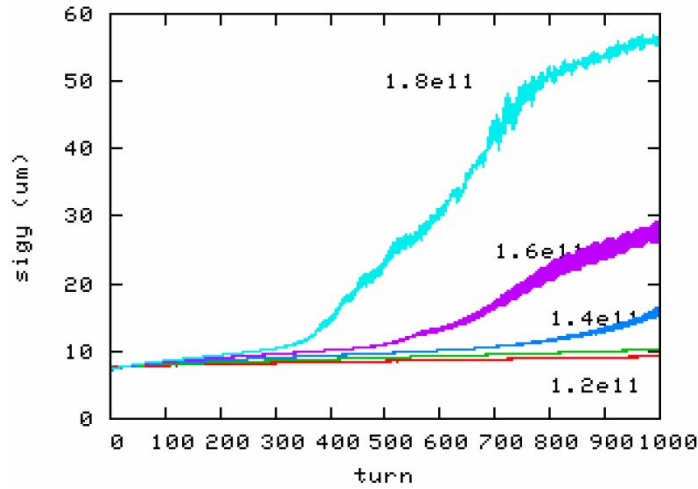
Figure 3: (K. Ohmi, KEK) Evolution of vertical positron beam size over 1000 turns in the ILC damping ring, for various densities of electron cloud. An instability threshold occurs for a cloud density between 1.2 and 1.4×10^{11} m^{-3}.
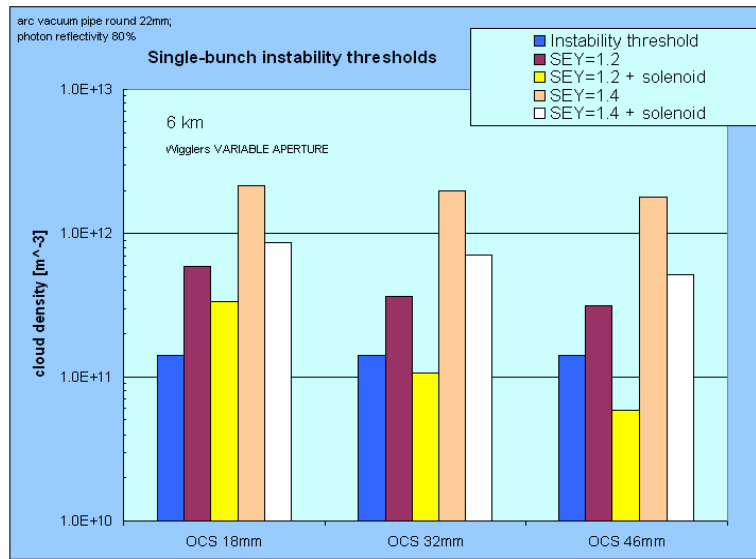
Figure 4: (M. Pivi, SLAC) Electron cloud density threshold (blue bar), compared with predicted average density under various conditions. The three groups show different wiggler apertures: 18 mm, 32 mm and 46 mm (left to right).

In the B-factories, solenoid windings around the vacuum chamber were effective at suppressing build-up of electron cloud in field-free regions. This technique may also be used in the ILC damping rings; however, the damping rings will have a relatively large proportion of their circumference within wiggler and dipole fields, so that even with all straight sections covered by solenoids there could remain enough electron cloud to drive instabilities in the beam. Other techniques being considered for suppression of electron cloud build-up in the damping rings include: coating the chamber surface with a material having a low secondary electron yield (such as titanium nitride, or titanium zirconium vanadium); shaping the surface with grooves to "trap" and re-absorb

secondary electrons before they can be accelerated by the beam; use of clearing electrodes. All these techniques show promising results in simulation; coatings and grooved surfaces have also been shown to reduce the effective secondary electron yield (SEY) in measurements performed in specialized apparatus. Experiments are underway to investigate the properties of low-SEY coatings and grooved surfaces in an accelerator environment at PEP-II [6] and initial results appear promising.

Predictions of the build-up of electron cloud and its impact on the performance of the damping rings are based on simulations. However, although the simulation codes have been benchmarked against data collected from existing machines, there remain significant extrapolations in the beam parameters from any existing storage ring to the ILC damping rings. For example, the vertical emittance specified for the damping rings is three orders of magnitude lower than that achieved in the B-factories. There are concerns that effects that could significantly limit the performance of the damping rings may not even be observable in machines with relatively much larger emittances. Therefore, a priority for the R&D program is to collect data at a facility that will: provide beam parameters (particularly, bunch charge, bunch spacing and emittances) and environment (vacuum chamber, wiggler fields) as close as possible to those specified for the damping rings; allow detailed measurements of cloud build-up and its impact on the beam; allow tests of a variety of mitigation techniques. Possibilities being considered for test facilities include CesrTA at Cornell University, and, on a longer timescale, KEKB.

While effects ascribed to electron cloud have been observed in electron machines, electron cloud is not expected to have a significant impact on performance of the electron damping ring. However, there are concerns that beam instabilities could be caused by accumulation of ions from residual gas in the vacuum chamber. At equilibrium, the small size of the beam means that only light ions can be trapped; however, the injected beam size is much larger, and even heavy ions can be trapped during the early stages of the damping process. Including regular gaps in the fill can prevent long-term ion trapping (though the gaps must be positioned so as to be consistent with the overall timing scheme of the ILC), but it is possible that sufficient ions can accumulate during the passage of even a small number of bunches to cause observable instabilities. Effects consistent with such a "fast ion" instability have been observed at the ALS [7], the PLS [8] and the ATF [9], though quantitative data are still lacking: fast ion effects are expected to become stronger as the beam size is reduced, and achieving the low-emittance regime specified for the damping rings is challenging. A theory to describe the fast ion instability has been developed by Raubenheimer and Zimmermann [10]; applied to the ILC damping rings, the theory predicts instability growth times of a few tens of turns, depending on the vacuum pressure. Modern bunch-by-bunch feedback systems are capable of suppressing instabilities with growth times of 20 turns or so, and recent simulation studies 11 suggest that a combination of a fast feedback system and low vacuum pressure (below 1 ntorr in the straights) will allow the damping rings to avoid limitations from ion effects.

Some other dynamics effects more usually associated with relatively low energy beams or hadron storage rings are of potential concern in the ILC damping rings because of the very low emittance regime in which the damping rings will operate. However, estimates made for the present design of the damping rings indicate that such effects should not limit performance. For example, the increase in horizontal emittance from intrabeam scattering will likely be of order 20%, which can easily be

accommodated by providing an appropriate margin in the lattice design. While it is still desirable to confirm predictions of collective effects such as space charge and intrabeam scattering by performing studies in machines operating as close as possible to the parameter regime of the damping rings, the top priorities for the ILC damping rings remain electron cloud and ion effects.

2.1.3   Preservation of Small Emittance in the RTML and Main Linacs

There are two main sources of emittance growth:
- wakefield effects, primarily in the superconducting linacs, but also from other apertures such as collimators;
- Chromatic (i.e. dispersive) effects, arising from magnet misalignment and beam trajectory errors.

One of the advantages of using superconducting RF is the relatively low cavity wakefields. The expected mechanically alignment accuracy of the accelerating cavities (a few hundred microns RMS) is good enough for suppressing single-bunch wakefield effect to acceptable levels. Multi-bunch wakefields are handled by random detuning (by fabrication errors) of the higher-order modes (HOM) in cavities at the 0.1% level, and by special purpose HOM couplers and absorbers.

Chromatic effects, however, require a typical quadrupole alignment accuracy which is one to two order-of-magnitude better than can be achieved with state-of-the-art mechanical alignment techniques. Beam-based alignment algorithms become mandatory to achieve the required emittance preservation (emittance growth budgets).

The two main sources of spurious dispersion are offset errors of quadrupole magnets and tilt errors of accelerating cavities, both of which effectively give a dispersive (i.e. energy-dependent) kick to the particles in a bunch. The kicks introduce a linear energy correlation in the transverse beam phase space (dispersion) resulting in a larger *projected* emittance, which if left locally uncorrected filaments as the beam is transported (accelerated in the linacs) down the machine. The focus of the single-bunch beam dynamics studies in these sections of the machine are primarily aimed at determining beam-based alignment techniques which achieve the required alignment accuracy (tolerable spurious dispersion). These techniques are generally based on measurements of the beam trajectory using Beam Position Monitors (BPMS). Additional 'global' tuning techniques, such as the application of closed-trajectory dispersive bumps or adjustment of combinations of quadrupoles to fine-tune the remaining linear aberrations require either a direct and accurate measurement of the beam emittance, or ultimately the luminosity itself.

Beam Based Alignment Techniques
There are several methods of beam-based alignment (correction) for suppressing dispersive effects which cause emittance growth. Here we discuss two examples: kick minimization steering (KMS) and dispersion free steering (DFS).

In KMS, we assume every quadrupole magnet has attached dipole correctors (one horizontal and one vertical) and an attached BPM. The sum of squares of total kick at the quadrupole-dipole,

$$\sum_i r^2 (y_i \pm \theta_i / k_i)^2 + \sum_i y_i^2 \,, \tag{4}$$

is minimized. The sign + is for horizontal and – for vertical plane. i is index of quad-dipole-BPM set, y_i the beam position (BPM reading), θ_i the kick angle of the dipole corrector, k_i the integrated normalized strength (inverse of the focal length) of the quadrupole magnet. Note that $\pm k_i y_i$ is the horizontal or vertical kick angle produced by the quadrupole magnet if there is no relative offset between the quadrupole magnetic field center and the BPM electrical center. The second term is necessary to *constrain* the absolute trajectory, preventing it from becoming too large (a general result in the presence of measurement errors); r is a weighting factor, which should be approximately equal to the ratio of the expected typical quadrupole misalignment and quadrupole-to-BPM offset error, the latter of which should be small for the algorithm to be effective. Accurate determination of the quad-to-BPM offset requires beam measurement, using a technique known as "quad shunting". In quad shunting, the strength of quadrupole magnets is changed one by one and the resulting difference in the downstream beam trajectory is measured. The difference trajectory is proportional to the strength of the quadrupole field and the beam offset with respect to the quadrupole field center.

DFS functions somewhat differently. The actual dispersive trajectory is measured directly by varying the beam energy. A corrected trajectory is found which minimizes the difference measured, and hence the dispersion. Usually, a long beam line is divided into several sections and the correction is done section by section starting at the upstream end of the machine and moving systematically down. The beam energy is modified by typically tens of percent by adjusting the accelerating RF. The dipole correctors are then adjusted to minimize

$$\sum_i w^2 (y_i - y_{0,i})^2 + \sum_i y_{0,i}^2 \tag{5}$$

where $y_{0,i}$ and y_i are beam position at i-th BPM for the on-energy (nominal) and off-energy beam trajectories respectively. As for KMS, the second term is again necessary to avoid large absolute trajectory displacements in the presence of measurement errors. For DFS, the weighting factor w is approximately the ratio of typical expected RMS BPM misalignment and BPM resolution.

Examples of Simulated Performance: Long Return Line (RTML)

The ~11 km long return line, which transports the 5 GeV beam from the Damping Ring to the end of the accelerator complex will require beam-based alignment. Simulations of KMS, assuming quadrupole RMS offset error of 300 μm, quadrupole RMS roll error of 300 μrad and BPM-to-Quad RMS offset error of 30 μm show that a normalized vertical emittance growth of about 2nm, (10% of the nominal emittance) can be achieved [12]. Figure 5 shows sensitivity to the BPM-to-Quad RMS error. The results indicate that an BPM-to-Quad offset of typically <50 μm is required. The residual (minimum) emittance growth is due to *x-y* coupling from the rolled quadrupoles.
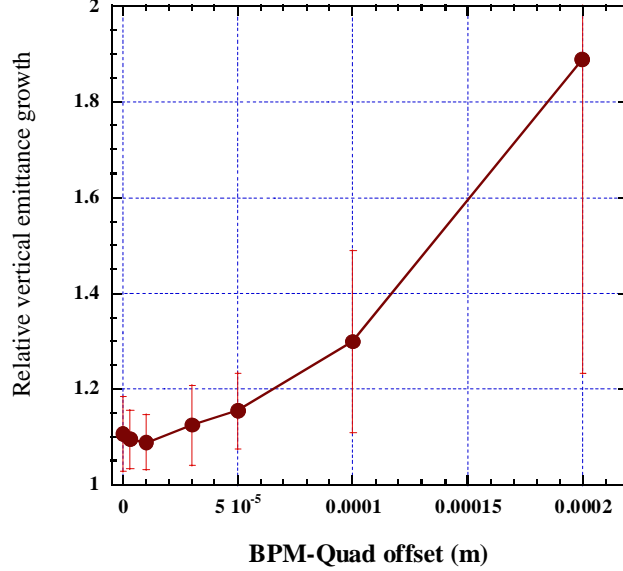
Figure 5: Vertical emittance at the end of the long RTML return line after KMS. as a function of BPM-to-quad offset error. (Averaged results over 100 random seeds.)

Examples of Simulated Performance: Turn around (RTML)

The 5 GeV 180° turn-around at the end of the return line has much stronger focusing to keep the horizontal dispersion small and hence reduce the effect of synchrotron radiation on the horizontal emittance. As a result, alignment tolerances are much tighter than in the turn-around. Preliminary simulations of KMS resulted in more than 20 nm expected vertical emittance growth (>100%). Adding 'global corrections' using dispersion bumps and coupling bumps have reduced this to ~4 nm, or 20%. These initial result are still not satisfactory and further studies are on going [13,14,15].

Examples of Simulated Performance: Bunch Compressors

The two bunch compressor sections required to reduce the bunch length by a factor of 30 may eventually prove to be the largest challenge for emittance preservation in the ILC. The long bunch lengths in the compressor linacs (9 mm in the first stage, 1 mm in the second stage) make increase the sensitivity to the expected random cavity tilts and wakefield effects. The large energy spread generated by the compressor RF (2.5% and 1.5% in the first and second compressor stages respectively) significantly increases the chromatic effects and hence tighten the required alignment tolerances.

One candidate tuning method in the bunch compressors is DFS. Since the beam is far from the crest of the RF (close to the zero-crossing in the first-stage compressor), it is particularly convenient to use a phase of adjustment to produce the required change in beam energy. The result of a simulation study is shown in Figure 6. In this simulation, beam trajectories were recorded at three RF phase settings: nominal phase ϕ_0, $\phi_0 + \Delta\phi$ and $\phi_0 - \Delta\phi$. The figure of merit to be minimized is now (see equation 4):

$$\sum_i w^2 (y_{+\Delta\phi,i} - y_{-\Delta\phi,i})^2 + \sum_i y_{0,i}^2 \qquad (6)$$

where $y_{\pm\Delta\phi,i}$ denote i-th BPM reading with phase setting of $\phi_0 \pm \Delta\phi$. The method was applied simultaneously to both the first- and second-stage compressors. This minimum result of 4 nm increase (20%) is good but still requires improvement [16, 17].
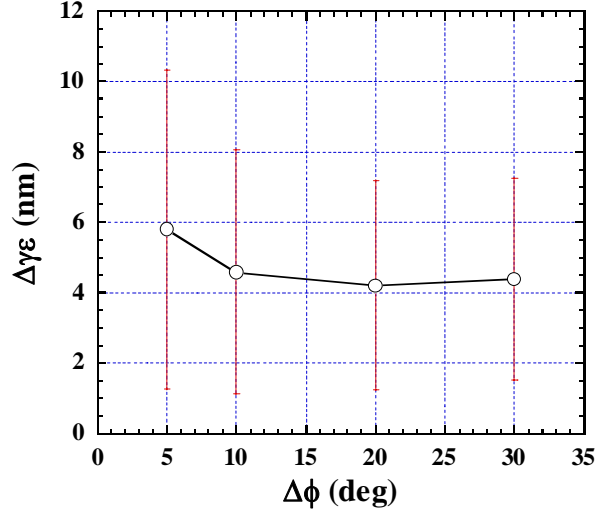
Figure 6: Vertical normalized emittance growth as function of phase change of DFS in the bunch compressors. Average of 50 random seeds (circles) and standard deviation (error bars) are shown. (The following random RMS errors were used; quad and bend magnet offset 150 μm, BPM-to-quad offset 7 μm, BPM resolution 1 μm, cavity offset 300 μm and cavity tilt 300 μr.)

Examples of Simulated Performance: 15-250 GeV 1.3 GHz Superconducting Main Linac

Low emittance preservation tuning in Main Linac has been intensely studied over the past decade by many people using many different computer codes. DFS is the most popular tuning method [18, 19, 20, 21, 22]. Results of DFS have been cross checked using various simulation codes [24]. KMS with an additional correction for cavity tilts has also been studied (although less extensively than DFS) with similar performance [25]. Here, we show example of DFS tuning studies [23].

Table 2: RMS alignment errors assumed for the Main Linac simulations. These values are considered as 'installation' alignment tolerances.

	Vertical	*Horizontal*
Quad offset w.r.t. design	0.36 mm	1.08 mm
Cavity offset w.r.t. design	0.64 mm	1.92 mm
BPM offset w.r.t. design	0.36 mm	1.08 mm
Quad roll w.r.t. design	0.3 mrad	
Cavity tilt w.r.t. design	0.3 mrad (pitch)	0.9 mrad (yaw)
BPM resolution	1 μm	1 μm

Table 2 shows the vertical and horizontal alignment errors assumed in the simulations. Figure 7 shows the resulting normalized vertical emittance along the Main Linac after DFS (assuming the errors in Table 2), averaged over 50 seeds.
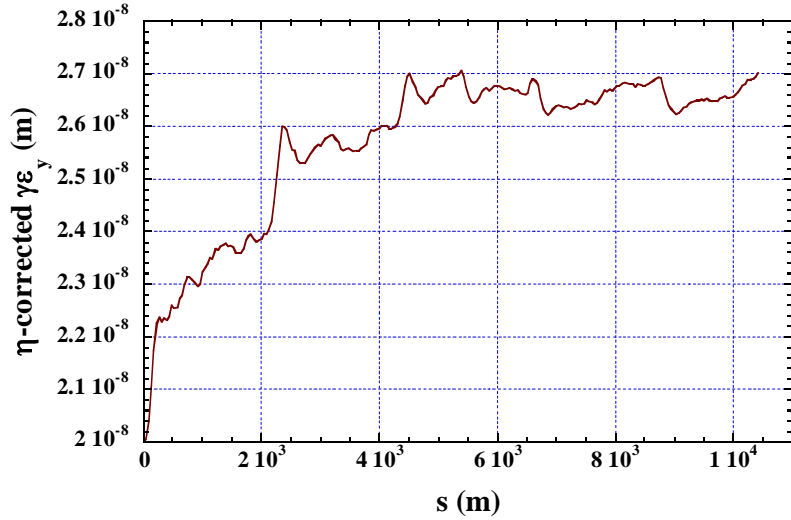
Figure 7: Normalized vertical emittance along Main Linac after DFS with the "standard" set of errors. Average of 50 random seeds.
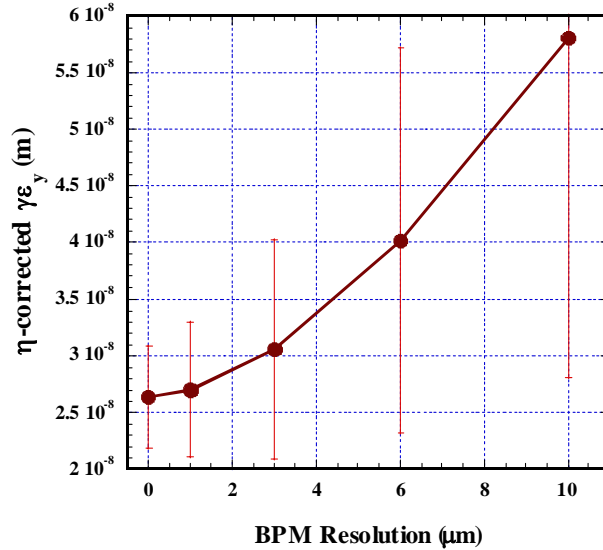

Figure 8: Effect of BPM resolution on the average vertical emittance after applying of DFS. (Data points are averaged over 40 seeds.)

The achievable performance for DFS is set by the BPM resolution. Figure 8 shows the effect of the BPM resolution (random noise) on the DFS performance. To keep the emittance growth below ~50% in the Main Linac would require a BPM resolution of ~3 μm or less (based on this simulation.) Note the residual emittance growth at zero resolution (~6 nm) is attributed to the remaining non-zero errors in Table 2.

The results shown in the above figures assume a linac which follows the curvature of the earth ($r \sim 6000$ km). This results in a small but nevertheless non-zero *design* vertical dispersion along the entire linac. The DFS algorithm was developed for 'laser-

straight' beamlines, where the design dispersion is zero (hence dispersion *free* steering). For the curved linac, the goal is to achieve the non-zero design dispersion: in this case we tend to refer to the modified algorithm as dispersion *matched* steering (DFM).

For the most part, the impact of the non-zero dispersion is negligible (providing it is correctly matched at the entrance and exit of the linac and that it is accounted for in the algorithm). One particular consequence is an increased sensitivity to the linear slope (or calibration) error of the BPMs. Figure 9 shows the influence of random BPM scale errors on DMS performance. Clearly a calibration better than ~10% is required, which is quite challenging. This effect can be easily understood. DFS is essentially a nulling technique: we simply do not want the beam to move when we change the energy. Here the scale errors only play a role in how fast the algorithm converges (i.e. the number of times we need to iterate). For DFM the beam moves with energy *by design*, and this motion must be accurately determined, and hence the scale error plays a significant role.
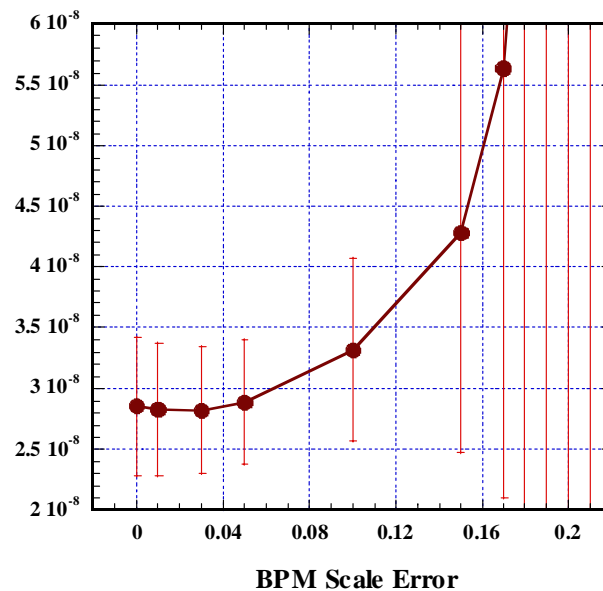
Figure 9: Impact of BPM linear scale error on DFS performance.
(Date points are averaged over 40 seeds).

Dynamic effects

KMS, DFS and DMS are all beam-based alignment techniques which have been developed to achieve the *static* alignment tolerances required for emittance preservation. The sensitivity to (predominantly) quadrupole motion due to vibration or slow ground motion drifts (or indeed other environmental effects such as temperature) requires attention to trajectory correction and almost constant beam tuning.

Both quadrupole vibration and power supply ripple will cause "beam jitter" (fast random transverse motion of the beam). In the Main Linac, a vertical quadrupole vibration of 100 nm cause approximately one beam sigma of vertical motion of the linac (entrance to the BDS), and scales linearly with the vibration amplitude. The emittance growth "jitter" associated with this amplitude of motion is negligible, but scales quadratically with the quadrupole vibration amplitude; an amplitude of ~200 nm begins to have a significant effect. Fortunately, we do not expect the quadrupoles to vibrate more than 100 nm inside the cryostats.

The beam motion would significant impact on the luminosity, however, if it were not for the use of fast intra-train beam feedback.

Apart from quadrupole vibration, there are other potential sources of potentially damaging beam jitter. One concern in the long transport line (return line) in the RTML, where time-dependent stray magnetic at the nTesla level may be an issue.

Again the ILC makes use of the long 1 ms ~3000 bunch train to correct an induced jitter. A feed-forward system utilizing the turnaround (monitoring orbit of each bunch before the turnaround and correct the orbit of that bunch after the turnaround), will mitigate most of accumulated beam jitter from the damping ring to the entrance of the bunch compressors. The remaining uncorrected effect is then the emittance growth. This is especially a problem for the jitter in the turn-around itself, where the strong focusing leads to a large chromaticity, and hence tight tolerances on both magnet position and beam stability (jitter).

One study has showed that vertical orbit jitter of one-sigma of the beam size in the turnaround causes emittance growth of about 1.6 nm, or 8% of nominal emittance. A random time-dependent stray magnetic field of 2 nTesla in the long transport line can induce such orbit jitter [26]. (Note this is only for fast variation which cannot be corrected by trajectory feedback leading into the turn-around.) Fortunately measurements of stray fields inside accelerating housings have shown weaker time-dependent amplitudes [27]. However, for confirmation, measurements at different places under similar conditions to the ILC beam tunnel are needed.
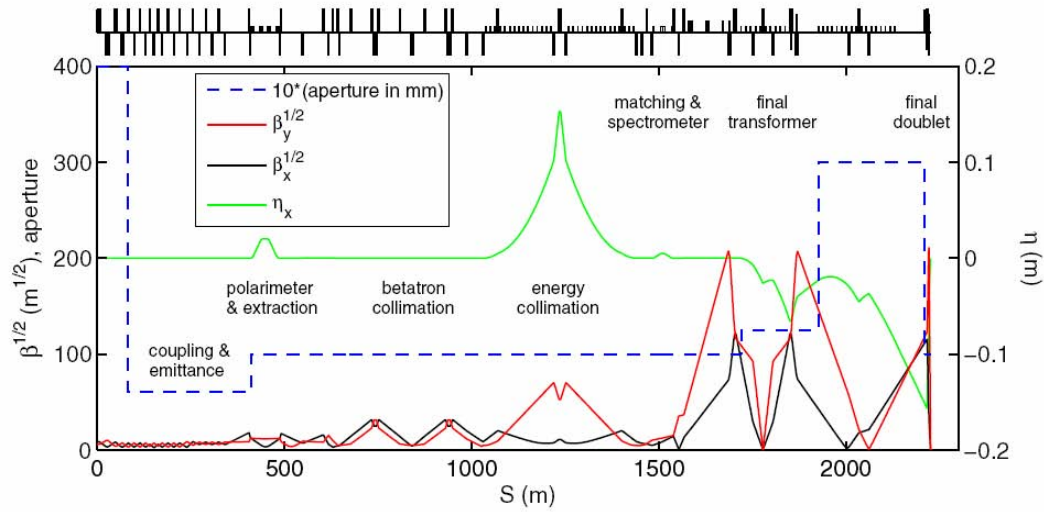
2.1.4 Beam Delivery System

Producing ILC luminosity requires colliding beams with nanometer scale sizes, which is the primary goal of Beam Delivery System. Consequent beam dynamics challenges include the need for strong focusing in the Final Focus part of BDS, compensation of chromaticity in the FF, careful compensation of nonlinear aberration in FF lattice and overcoming synchrotron radiation driven emittance growth arising in the bends, quadrupoles and other magnets of BDS. The small beam sizes at the interaction point (IP) and small beam emittance produce particular requirements on stability of the elements and on the design of feedback systems and tuning methods. The Beam Delivery must also provide acceptable background conditions for the experimental detectors, the innermost vertex detector of which has a radius of only 1.2-1.5 cm. Providing acceptable background would require avoiding even a single particle of the beam hitting any apertures in the Interaction Region (IR), requiring high-efficiency collimation of the unavoidable beam halo which accompanies the beam core at large apertures. The relatively small gaps of spoilers and absorbers of the collimation system may create wake-fields and an emittance growth for off-centered beam; use of non-linear magnets (such as octupoles) to effectively fold in the high-amplitude tails of the halo may allow the widening of the spoiler gaps in the collimation sections, thus alleviating the wake-field effects.

Addressing stability of the BDS beamline would require constant tuning of various knobs, to prevent decay of the luminosity, and also requires careful measurement of the beam properties (phase space) as it comes out of the linac. The current 14 mrad crossing-angle at the IP needs to be compensated with use of crab-cavities, which rotate the beam before collision but must not perturb the beam quality due to various beam-induced parasitic modes excited in the cavities themselves. The solenoid field of the

experimental detector, which overlaps with quadrupole field of the final focusing magnets, produces anomalously large coupling of the beam, which must be compensated. As a final example, the resistive wall wake-fields of the vacuum chamber are capable of deteriorating the beam emittance, if the chamber is not accurately aligned to the beam. There are many other challenges in the design of Beam Delivery system, related to extracting highly disrupted beam, providing machine protection functions, arranging Interaction Region configuration for two push-pull detectors, providing precise beam energy and polarization measurements *etc.*, which are beyond the scope of this beam dynamics focused article.

The Beam Delivery design and beam dynamics challenges mentioned above are addressed in the system outlined in Figure 10, where the optics and functions of BDS are shown. The main subsystems of the Beam Delivery starting from the exit of the main linac are the diagnostics region, betatron and energy collimation, final focus, interaction region (IR) and extraction line. The initial part of the BDS is responsible for measuring and correcting the properties of the beam before it enters the collimation and FF. The skew correction section and the emittance diagnostic section contain four skew quadrupoles and also four laser wires which are capable of measuring horizontal and vertical RMS beam sizes down to 1 micrometer. Such system allows a complete measurement of 2D transverse phase space and determination of the projected horizontal and vertical emittances and correction of any arbitrary linearly coupled beam. Particles in the beam halo are removed in the BDS collimation system consisting of betatron collimation section followed by energy collimators. The collimators are arranged in spoiler-absorber pairs where the spoilers have typical full gap of about 1mm, and are tapered, to reduce wake-fields. Electromagnetic showers created by primary beam particles in the collimators produce penetrating muons which can easily reach the collider hall. The muon flux through the detector is reduced by five-meter-long tunnel-filling magnetized iron shield located several hundred meters upstream of the collision point. The Final Focus system de-magnifies the beam to the required size and provides local chromaticity correction using sextupoles next to the final doublets [28]. The final focus includes two superconducting octupole doublets which use nonlinear focusing to reduce the amplitudes of beam halo particles while leaving the beam core untouched. This "tail-folding" would permit larger collimation aperture that in turn would reduce the amount of beam power intercepted in the collimators and the unwanted wakefields [29]. The Beam Delivery system is designed for 500 GeV CM and can reach up to 1 TeV CM in the same layout, with additional magnets installed in the provided gaps. Below we will review some of the design features and associated beam dynamics challenges in more detail.

Figure 10: Beam Delivery optics and subsystems. The system is designed to work up to the energy of 1 TeV in the center of mass in the same layout.

The layout of magnets in the Final Doublet of the Interaction Region of the BDS is shown in Figure 11. The 14 mrad crossing angle dictates the use of compact design of the superconducting magnets. The local compensation of chromaticity is done with sextupoles SD0 and SF1 embedded in the Final Doublet. The first quadrupoles in the FD are built with use of active shielding design – a negative polarity quadrupole coil compensates the fringe field outside of the magnet, thus reducing cross-talk between the incoming and outgoing beamlines. The magnets of the Final Doublet are arranged in two independent cryostats, with warm space in between – this is the area where beampipe will be disconnected in the push-pull operation foreseen for the two detectors.
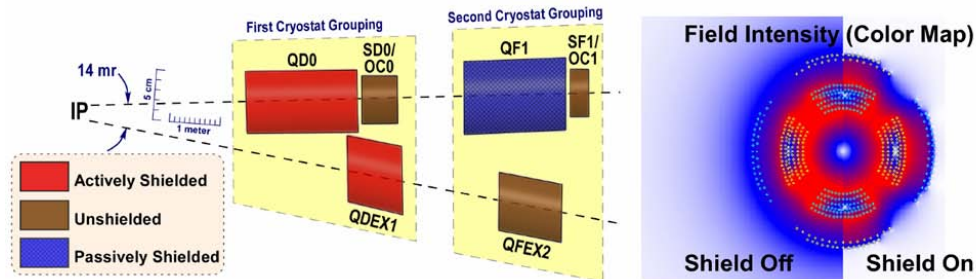
Figure 11: Layout of the BDS Interaction Region magnets, quadrupoles QD0 and QF1 and sextupole-octupole packages SD0/OC0 and SF1/OC1 for the incoming beam and quadrupoles QDEX1/2 for the outgoing beam. Active shielded quadrupoles is illustrated on the right. The passively shielded quadrupoles use iron layer for the shielding.

The design and beam dynamics of the Interaction Region is complicated by the presence of the detector's 3-5 Tesla solenoid field, which overlaps with the Final Doublets, in particular the QD0 quadrupole. The overlap of the solenoid and quadrupole field breaks the symmetry of the solenoid field and create anomalously large coupling of the beam, which is many tens of times larger than the same solenoid would produce

if there would be no overlap with quadrupoles. Such coupling could be compensated efficiently and locally with use of a weak antisolenoid, with optimized field shape [30]. The antisolenoid is weak in the sense that it compensates only the part of detector solenoid field which overlaps with the FD, and not the full integral. Such compensation is illustrated in Figure 12. An interesting and helpful feature of such local compensation is that it practically independent on beam energy or optics settings, and therefore would not require retuning in normal operation. In the most recent design of the FD, the antisolenoid is incorporated into the QD0 cryostat in a force-neutral double solenoid configuration [31], which eliminates the force acting on the compensating solenoid from the main solenoid of the detector.
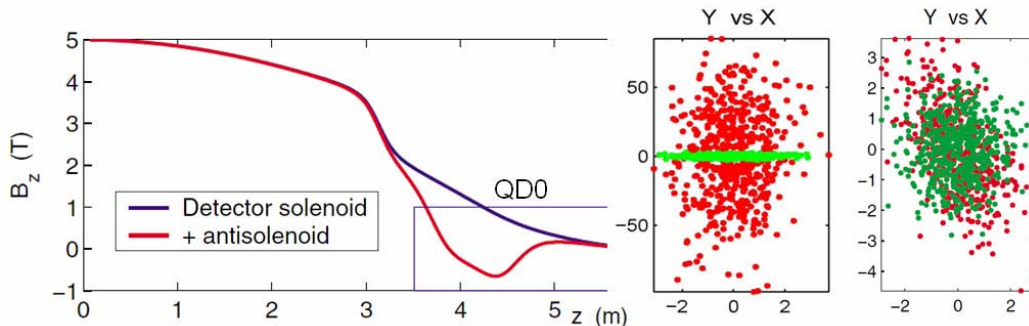
Figure 12: Example of the overlap of detector solenoid field with Final Doublet quadrupole QD0. The field overlap produces the anomalously large beam coupling illustrated in the middle picture, in normalized X-Y plane. Green and red dots show the tracked beam, without and with the solenoid effects. Coupling can be compensated locally, with use of antisolenoid, which removes major part of the coupling as shown on the right picture.

The Beam Delivery collimation system must collimate the beam tails outside of 8-10 sigma in horizontal and 60-80 sigma in the vertical plane, in order to protect IR apertures from hits by any beam particles, or any synchrotron radiation photons generated by the beam halo. The beam sizes in the location of spoilers are enlarged to provide survival of spoilers after an accidental hit by a bunch, which determines the size of the gaps of the spoilers to be about a millimeter. Geometric and resistive wake-fields from narrow collimators are one of the challenges of the design not only because they create single bunch emittance growth for off-centered bunch and amplify beam jitter, but also due to challenges of accurate predictions of these effects. Computation of wakefields from shallow angle tapered collimators represent significant challenge, both for analytical and computer models, which is one of the reason for ongoing experimental program to measure collimation wakes for spoilers of various shapes and materials [32]. With the present design of the collimation system, ~0.5σ vertical beam jitter would result in approximately 5% emittance growth due to collimation wakefields. One of the possible ways to open the gaps of spoilers and reduce the effect of collimation wakefields is the use of so called octupole doublets to fold the tails of the beam halo [29]. These doublets apply nonlinear focusing, affecting the beam halo at large amplitudes, while leaving the beam core untouched. Two opposite polarity octupoles are arranged in pairs such that their overall combined effect gives focusing in all directions as illustrated in Figure 13. Two superconducting octupole doublets are installed in the beginning of Final Focus to allow folding of tails by a factor of three, in

terms of particle amplitudes in the Final Doublet, and thus provide an additional safety factor for collimation system.
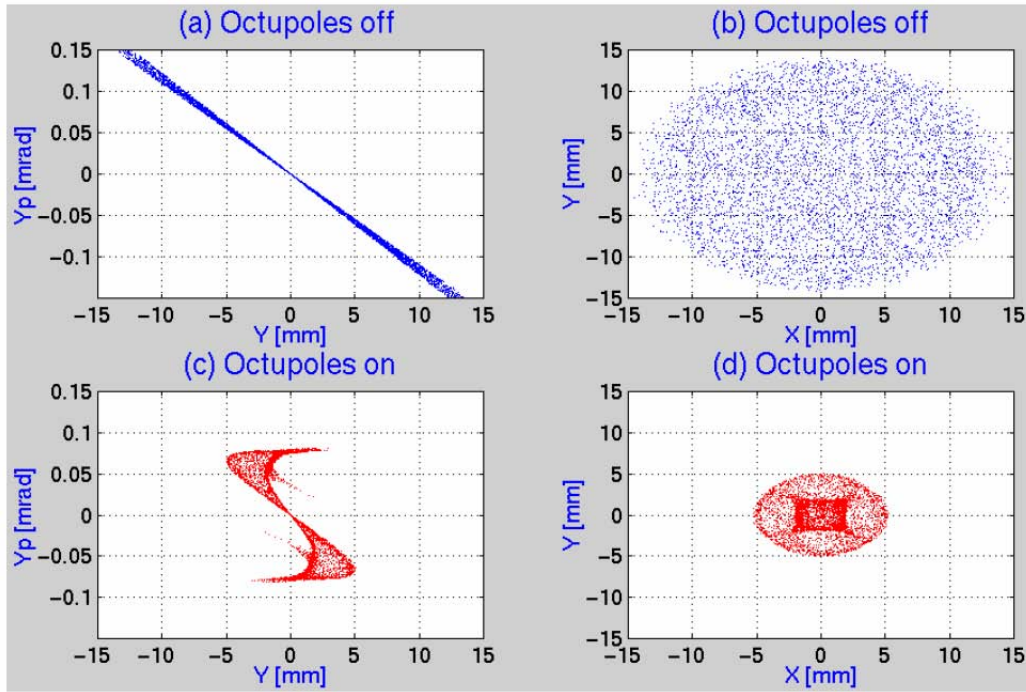

Figure 13: Tail folding effect of the octupole doublets on beam halo, as illustrated by the beam distribution at a beta-function maximum point in the Final Focus after the octupole doublets.

Maintaining the stability of the BDS is an essential prerequisite to producing luminosity. Since the beams have RMS vertical sizes of 5.7 nm at the IP, vertical offsets of about 1 nm will noticeably reduce the luminosity. In addition, especially for parameter sets with higher disruption, the beam-beam interaction is so strong that the luminosity is extremely sensitive to small variations in the longitudinal shape of the bunch caused by short-range wakefields. Beam-based orbit feedback loops are used to maintain the size and position of the beam at the IP. All of the feedback loops use beam position monitors with at least micron-level (and in some cases sub-micron) resolution to detect the beam position, and dipole magnets or stripline kickers to detect the beam. There are two basic forms of feedback in the BDS: train-by-train feedbacks, which operate at the 5 Hz repetition rate of the ILC, and intra-train feedbacks, which can apply a correction to the beam between bunches of a single train. A train-by-train feedback with several correctors controls the orbit through the sextupoles in the horizontal and vertical planes, where the optical tolerances are tightest. Additional correctors throughout the BDS help reduce long-term beam size growth. The orbit control feedback can maintain the required beam sizes at the IP over periods from a few hours to several days depending on details of the environment. On longer timescales, IP dispersion and coupling knobs need to be applied. The intra-train feedbacks use the signals detected on early bunches in the train to correct the IP position and angle of subsequent bunches. The offset of the beams at the IP is determined by measuring the deflections from the beam-beam interaction; this interaction is so strong that nm-level offsets generate deflections of tens of microradians, and thus BPMs with micron-level

resolution can be used to detect offsets at the level of a fraction of a nanometer. Corrections are applied with a stripline kicker located in the incoming beamline between SD0 and QF1.

The challenge of tuning the Beam Delivery system and maintaining the very small beam size reliably and for a long time is one of the motivations for creating the Beam Delivery test facility ATF2 at KEK, Japan [33]. The ATF2 is a small scaled down version of the ILC Beam Delivery system which will use 1.28 GeV beam extracted from ATF damping ring and focus it into 35-40 nm beam size. Layout of the ATF2 facility is shown in Figure 14.
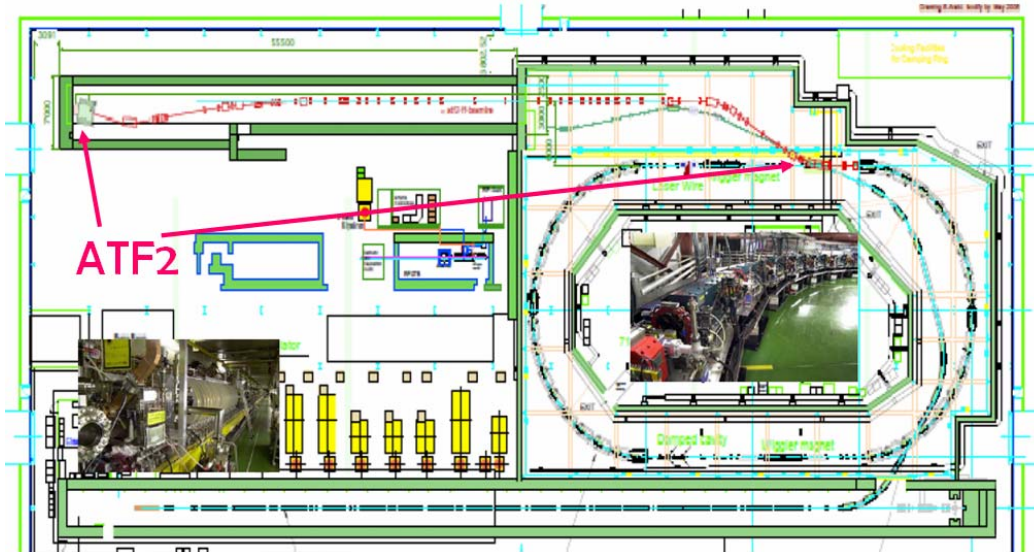
Figure 14: Layout of the ATF facility at KEK, Japan, where the ATF2 beam delivery test facility (shown by red) is being constructed

Maintaining the stability of ATF2 beam size will be done in a very similar way as is foreseen for the ILC BDS, with application of orbit feedbacks and sextupole tuning knobs. However an obvious complication is the absence of the opposite beam which provides IP beam position signal based on beam-beam effects and also the absence of a fast luminosity monitor. Those essential functions will be provided by nanometer resolution beam position monitor and a Shintake beam size monitor [34]. The large number of pulses required to obtain statistically significant measurement of the beam size is one of the challenges which makes tuning of the ATF2 beamline at least of the same complexity as ILC BDS. The intra-train feedback will also be studied in ATF2, when the multi-bunch mode (about sixty bunches) will become available.
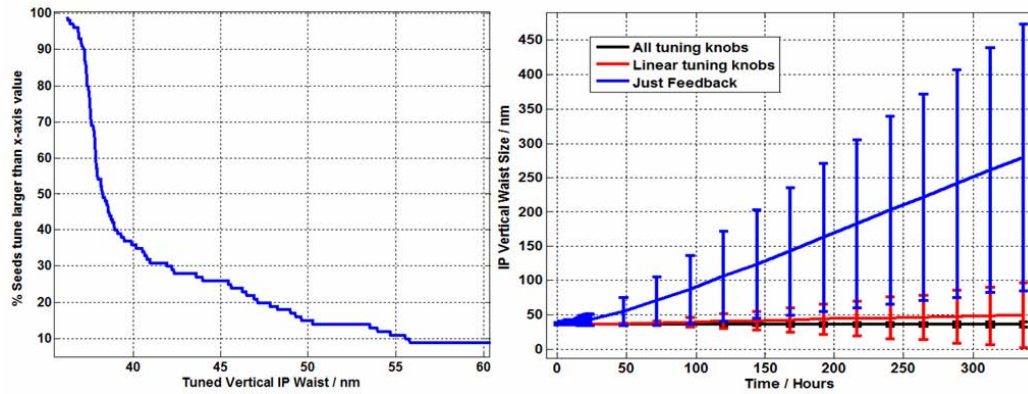
Figure 15: (Glen White, SLAC) Illustration to the working progress for the tuning study of ATF2 beamline. On the left, the histogram which shows the number of cases that achieved certain vertical beam size. For example, 65% of the cases reach beam size smaller than 40nm. The expected errors of magnets, position, beam position and energy jitter, resolution of instrumentation, etc. are taken into account. On the right, behaviour of the IP beam sizes is shown for the case of orbit feedback only and also for the case when linear and second order knobs are applied, which then able to keep the beam size constant for long time.

Extensive studies of ATF2 tuning are being conducted now. The studies (simulations) currently being implemented for ATF2 are now including 'real-world' practical details (by necessity) that have hitherto not been included in the ILC simulations. For example the limits of the movers, beamline apertures and radiation conditions caused by loss of a fraction of the beam during tuning. An example of tuning studies for ATF2 is shown in Figure 15. Commissioning of the ATF2 is planned to start in autumn of 2008.

2.1.5 References

1. The ILC Reference Design Report: http://www.linearcollider.org/cms/?pid=1000437 (2007)
2. A. Wolski, J. Gao, S. Guiducci (editors), "Configuration Studies and Recommendations for the ILC Damping Rings," LBNL-59449 (February, 2006).
3. C.E. Mitchell and A. J. Dragt, "Computation of Transfer Maps from Magnetic Field Data in Wigglers and Undulators," ICFA Beam Dynamics Newsletter, No. 42, pages 65-70 (April, 2007).
4. Y. Honda et al, "Achievement of Ultralow Emittance Beam in the Accelerator Test Facility Damping Ring," Phys. Rev. Lett. 92, 054802-1 (2004).
5. For reviews of some recent work on electron cloud effects, including studies related to the ILC damping rings, see the proceedings of ECLOUD 2007, Daegu, Korea (April, 2007). http://chep.knu.ac.kr/ecloud07/
6. M. Pivi, "Clearing Electrodes and Groove Tests Planned for the ILC DR Magnet Regions," proceedings of ECLOUD 2007, Daegu, Korea (April, 2007).
7. J. Byrd et al, "First Observations of a Fast Beam-Ion Instability," Phys. Rev. Lett. 79, 79-82 (1997).
8. J.Y. Huang et al, "Direct Observation of the Fast Beam-Ion Instability," Phys. Rev. Lett. 81, 4388-4391 (1998).
9. Y. Honda, "Pressure Dependence Studies of Multi-Bunch Beam," presented at ISG XI, KEK (December 2003). http://lcdev.kek.jp/ISG/ISG11/DR/FI_Honda.pdf

10. T.O. Raubenheimer and F. Zimmermann, "Fast Beam Ion Instability: Linear Theory and Simulations," Phys. Rev. E 52, 5487-5498 (1995).
11. E.-S. Kim, "Simulations of Fast Ion Instability in the ILC Electron Damping Ring," ICFA Beam Dynamics Newsletter, No. 43, pages 14-18 (August 2007).
12. K. Kubo, "Simulation of Low Emittance Transport in Long Straight Line of ILC RTML," ILC-NOTE-2007-008 (2006)
13. J. Smith, "Coupling Correction in the ILC Ring to Main Linac," ILC-NOTE-2007-006 (2007)
14. P. Tenenbaum, "Application of Kick Minimization to the RTML `Front End'," SLACTN-07-002 (2007).
15. P. Tenenbaum et.al., "Emittance Preservation in the International Linear Collider Ring to Main Linac Transfer Line." Contributed to Particle Accelerator Conference (PAC 07), Albuquerque, New Mexico, 25-29 Jun 2007.
16. P. Tenenbaum, "Emittance Studies in the 2006 Bunch Compressor," ILC-NOTE-2007-003 (2007)
17. Andrea Latina, to be published.
18. N. Walker, EUROTeV-Report-2005-017 (2005).
19. A. Latina et al., EUROTeV-Report-2006-050 (2006).
20. K. Ranjan et al., MOP064, LINAC 2006(2006).
21. K. Kubo, ILC-Asia Note 2005-25, ILC-Asia Note 2005-23 (2005).
22. Eliasson and D. Schulte, EUROTeV-Report-2005-021 (2005). (bumps in ML)
23. Kubo, ILC-Asia Note 2006-04 (2006)
24. J. Smith et.al., "Comparison of Tracking Codes for the International Linear Collider" Contributed to Particle Accelerator Conference (PAC 07), Albuquerque, New Mexico, 25-29 Jun 2007.
25. K. Kubo, ILC-Asia Note 2005-18, ILC-Asia Note 2005-17 (2005).
26. K. Kubo, "Rough Estimation of Fast-Changing Stray Field in Long Transport of RTML," ILC-NOTE-2007-007 (2006).
27. J. Frisch et al., SLAC-TN-04-041 (2004).
28. P. Raimondi and A. Seryi, ``A novel final focus design for future linear colliders," Phys. Rev. Lett. 86, 3779 (2001).
29. R. Brinkmann, P. Raimondi, A. Seryi, ``Halo reduction by means of nonlinear optical elements in the NLC final focus system," SLAC-PUB-8896, PAC 2001.
30. Y. Nosochkov and A. Seryi, ``Compensation of detector solenoid effects on the beam size in linear collider", Phys. Rev. ST Accel. Beams 8, 021001 (2005).
31. B.Parker, et al., ``The Superconducting Magnets of the ILC Beam Delivery System," SLAC-PUB-12832, also PAC 2007.
32. N.K. Watson, et al., ``Direct measurement of geometric and resistive wakefields in tapered collimators for the International Linear Collider," EUROTEV-REPORT-2006-059.
33. ATF2 proposal, vol. 1 and 2, SLAC-R-771, SLAC-R-796, KEK-REPORT-2005-2, KEK-REPORT-2005-9.